Arctic, Antarctic, and Alpine Research, Vol. 40, No. 1, 2008, pp. 148–160

Spatial Reconstructions and Comparisons of Historic Snow Avalanche Frequency and Extent Using Tree Rings in Glacier National Park, Montana, U.S.A.

*B. A. Reardon**
G. T. Pederson†
C. J. Caruso† and
D. B. Fagre‡

*Corresponding author: U.S. Geological Survey Northern Rocky Mountain Science Center, Global Change Program, Science Center, Glacier National Park, West Glacier, Montana 59936, U.S.A.
blase.reardon@gmail.com
†Big Sky Institute, 106 AJM Johnson Hall, Montana State University, Bozeman, Montana 59717, U.S.A.
‡U.S. Geological Survey Science Center, West Glacier Field Station, Glacier National Park, West Glacier, Montana 59936, U.S.A.

Abstract

Natural snow avalanches have periodically damaged infrastructure and disrupted railroad and highway traffic at the southwestern corner of Glacier National Park, Montana. The 94-year history of these disruptions constitutes an uncommon record of natural avalanches spanning over nine decades and presents a unique opportunity to examine how natural avalanche frequency and minimum extent have varied over time due to climatic or biophysical changes. This study compared the historic record of natural avalanches in one avalanche path with tree-ring evidence of avalanches from 109 cross sections and increment cores collected in the same path. Results from combined historic and tree-ring records yielded 27 avalanche years in the 1910–2003 chronology, with the historic record alone underestimating avalanche years by half. Mean return period was 3.2 years. Interpolated maps allowed for more spatially precise estimates of return periods throughout the runout zone than previous studies. The maps show return periods increase rapidly downslope from 2.3 to 25 years. Avalanche years were associated with positive Snow Water Equivalent anomalies at a nearby snow course. Minimum avalanche extent was highly variable but not associated with snowpack anomalies. Most avalanche years coincided with years in which the mean January–February Pacific Decadal Oscillation (PDO) and El Niño–Southern Oscillation (ENSO) 3.4 indices were neutral. The findings suggest that changes in Pacific climate patterns that influence snowfall could also alter the frequency of natural snow avalanches and could thus change disturbance patterns in the montane forests of the canyon.

DOI: 10.1657/1523-0430(06-069)[REARDON]2.0.CO;2

Introduction

Natural snow avalanches are physical processes that regularly disturb mountain ecosystems in the U.S. Northern Rocky Mountains. Snow avalanches scour trees from avalanche paths, providing space for herbaceous and woody species to establish. The resulting avalanche paths alternate with montane forests across a slope, creating complex vegetation patterns with manifold structures and functions (Patten and Knight, 1994). Avalanche paths transfer nutrients from high mountain ridges and catchments to valley bottoms (Butler et al., 1992) and can act as fuel breaks for forest fires moving laterally across mountain slopes (Malanson and Butler, 1984), further diversifying the mosaic of vegetation. The extensive edges of this mosaic provide diverse habitat for wildlife. Bird species abundance is high and, in the Glacier National Park (GNP) region, many mammals rely on food sources in avalanche paths, with grizzly bears (*Ursus arctos horribilis*) preferentially foraging in avalanche paths in spring, summer, and fall (Mace and Waller, 1997). For species that use these paths in the winter, such as elk (*Cervus elaphus*), wolverine (*Gulo gulo*), and bighorn sheep (*Ovis canadensis*), avalanches can be a significant cause of mortality (Butler, 1986; R. Yates, personal communication, 2006; K. A. Keating, personal communication, 2006). The dense snow of avalanche debris can supply meltwater to streams after seasonal snow at similar elevations has melted. This debris can also obstruct streams (Martinelli, 1984; Butler, 1989), and avalanche-deposited woody debris can serve as a source of dissolved organic carbon (Walsh et al., 2004).

Snow avalanches also pose a hazard to human activities and structures that cross avalanche paths (Mears, 1992). In John F. Stevens Canyon, at the southwestern corner of GNP, Montana (Fig. 1), avalanches have damaged infrastructure and disrupted railroad and highway traffic since at least 1910 (Reardon et al., 2004). Among the most severe accidents are the deaths of three railroad workers in 1929, the burial of two highway workers in 1950, extensive damage to several snowsheds and a locomotive in 1956 and 1957, the destruction of a highway bridge in 1979, and the derailment of a freight train in 2004 (Reardon et al., 2004).

Using an Avalanche Hazard Index (Schaerer, 1989), Hamre and Overcast (2004) calculated that the risk from avalanches in Stevens Canyon is similar to or exceeds that of numerous transportation corridors in western North America. In most other corridors, managers have instituted avalanche hazard mitigation programs that include the use of explosives to artificially trigger avalanches, which can change the frequency and extent of avalanches (Martinelli, 1974; Fitzharris and Schaerer, 1980; McClung and Schaerer, 1993). In Stevens Canyon, however, avalanche hazard mitigation was limited to nine snowsheds until 2004, when an avalanche forecasting program was established. The avalanche history in Stevens Canyon thus constitutes a nine-decade record of natural avalanches that is uninfluenced by explosives use. This combination is uncommon in western North

© 2008 Regents of the University of Colorado
1523-0430/08 $7.00

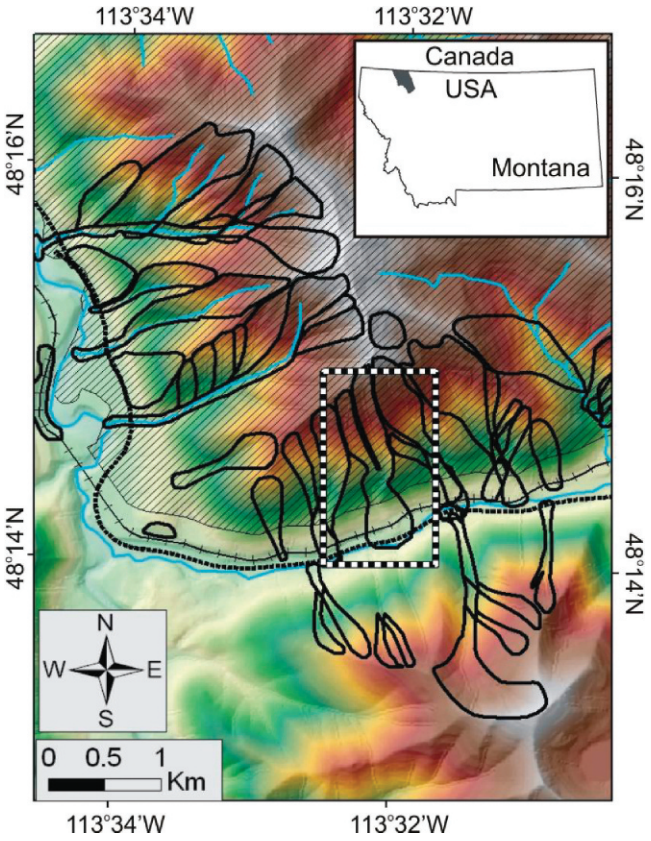

FIGURE 1. The Shed 10.7 avalanche path (outlined by the black and white square) is located in the southwestern corner of Glacier National Park, Montana, U.S.A. (crosshatched area). The path is generally south-facing, and the run-out zone crosses the Burlington Northern Santa Fe Railroad (single hatched line) and U.S. Highway 2 (thick dashed line). Some nearby avalanche paths in the area are also shown.

America, and Stevens Canyon presents a unique opportunity to examine how natural avalanche frequency and extent have varied over time due to climatic or biophysical changes.

The quality of the historic record is both an aid and an obstacle to such an effort. In most mountain areas in Montana, human presence in the winter was at best irregular for most of the 20th century, and nearly all natural avalanches went unrecorded. In Stevens Canyon, however, the transportation infrastructure allowed people, chiefly railroad and highway workers, to regularly observe and record natural avalanches throughout a winter. Unfortunately, the lack of a formal avalanche mitigation program meant that these observations were not documented consistently or systematically.

To improve the avalanche record, we developed a tree-ring-based chronology of avalanche events for one path in Stevens Canyon. Tree-ring-based records of avalanche events are an accepted supplement to, or substitute for, historic records because they can supply information about the characteristics of avalanches and other geomorphological processes (McClung and Schaerer, 1993; Stoffel, 2006). Trees record injuries from avalanche debris in their annual rings as scars or atypical growth patterns; these can be dated at an annual resolution and used to determine the frequency and minimum runout of snow avalanches (Burrows and Burrows, 1976; Carrara, 1979; Jenkins and Hebertson, 2004). In North America, tree-ring analyses have been conducted at scales ranging from a single avalanche path (Carrara, 1979; Jenkins and Hebertson, 2004) to multiple avalanche paths in multiple drainages (Butler and Malanson, 1985b; Jenkins and Hebertson, 1994; Rayback, 1998; Dube et al., 2004) and linked with larger synoptic climate patterns, such as El Niño–Southern Oscillation (ENSO) (Hebertson and Jenkins, 2003) and anomalous snowfall (Dube et al., 2004). In Europe, tree-ring-based chronologies have been used to reconstruct the frequency and extent of landslides, debris flows, and other geomorphological processes (Braam et al., 1987; Fantucci and Sorriso-Valvo, 1999; Stefannini,

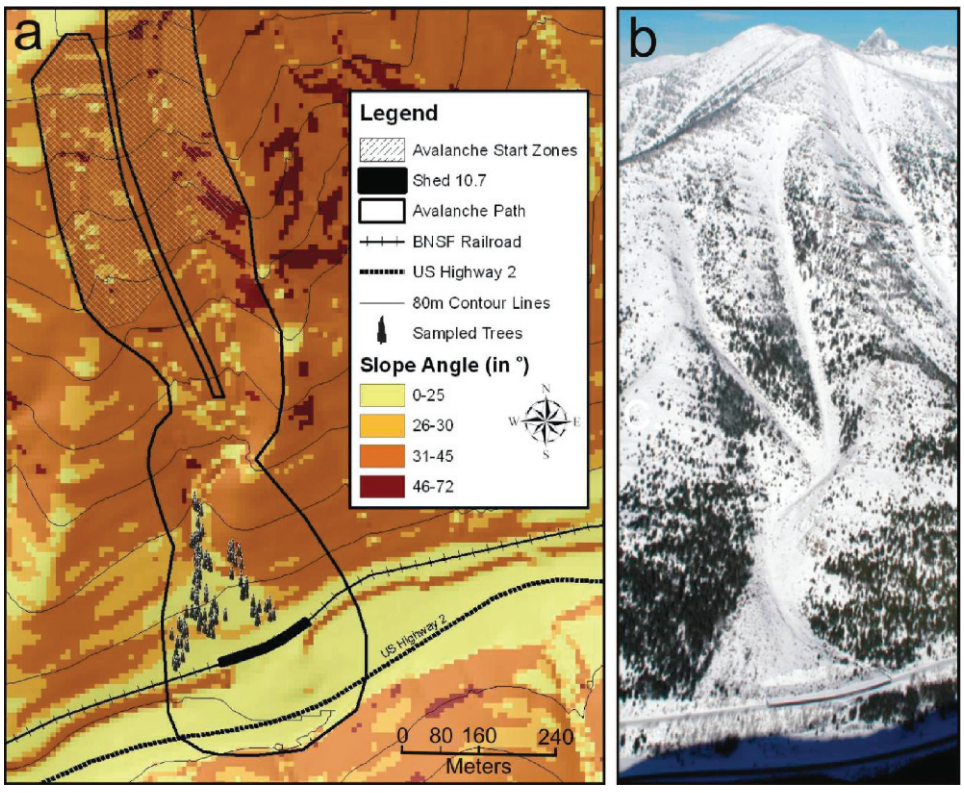

FIGURE 2. Map of (a) slope angles and tree sampling area above Shed 10.7 and U.S. Highway 2, and (b) oblique photo of shed 10.7 avalanche path. Photo by Darwon Stoneman, January 2004.

2004). Many of these span multiple centuries (Baumann and Kaiser, 1999; Stoffel and Beniston, 2006; Stoffel et al., 2006), much longer than most North American chronologies.

In Stevens Canyon, Butler and Malanson (1985a, 1985b) and Hamre and Overcast (2004) used tree rings to develop general avalanche chronologies for one or more avalanche paths. However, these chronologies were limited by restricted sample sizes or locations, and a reliance on increment cores. To establish a benchmark avalanche chronology against which other avalanche information in the canyon can be compared, we conducted intensive studies in one avalanche path.

Our objectives were to (1) expand the chronology of natural avalanches in John F. Stevens Canyon, (2) evaluate the accuracy of the existing historic chronology by comparing documented natural avalanches in one avalanche path with a high-resolution tree-ring record from the same path, (3) calculate both frequency and minimum extents of natural avalanches within a single avalanche path, and (4) evaluate climate factors that may influence the frequency and extent of natural snow avalanches in Stevens Canyon.

Study Site

The study site—the Shed 10.7 avalanche path—is one of several dozen major avalanche paths that threaten railroad and highway infrastructure and traffic in Stevens Canyon; it is named for the 205-m-long snowshed in its runout zone that partially protects the Burlington Northern Santa Fe Railway (BNSF). It was selected because destructive avalanches in the 2001/2002 and 2002/2003 winters killed or injured dozens of trees, yet left the stems and boles *in situ* or within several meters of their original position. The numerous dead trees allowed destructive sampling (tree cross sections and wedge samples of impact scars), which provides the most reliable identification and dating of avalanche-induced tree responses (Carrara, 1979). Also, the fact that the trees remained *in situ* enabled precise recording of each sample location using a hand-held GPS unit, which in turn allowed mapping of sample size, minimum avalanche extent in a given winter, and estimated avalanche frequencies within the runout zone.

The Shed 10.7 avalanche path (Figs. 2a, 2b) lies on the steep southern slopes of Running Rabbit Mountain (2347 m a.s.l.). The main start zone lies between 2070 and 2190 m a.s.l. (Hamre and Overcast, 2004). The track is steep and confined, with an S-curve at the bottom. Below the curve, the path transitions abruptly into a broad, fan-shaped runout zone cut longitudinally by a shallow, treeless gully. The snowshed and railroad cross the bottom of this fan at 1270 m a.s.l. The slope drops steeply from the railroad to U. S. Highway 2, which runs through the floodplain of Bear Creek at 1235 m a.s.l. Total vertical fall from the main start zone to Bear Creek is 955 m, with an alpha angle of 27°. A tributary start zone and track run just west of the main path. The tributary track falls 450 vertical m to a confluence with the main track just above the bottom of the S-curve.

The surfaces of both start zones and tracks are primarily grasses, herbaceous plants, and small shrubs with some exposed mineral soils and small rock outcrops. There are no rock faces, talus piles, scree slopes or unconsolidated morainal deposits that might provide a source for consistent or widespread rockfall or debris flows. The runout zone surface is covered with a mix of large shrubs, standing trees, downed trees, and woody debris. Many trees within the runout zone exhibit signs of damage from multiple avalanche events. The trimline along the western edge is abrupt, while along the eastern edge, the transition from avalanche path to forest is more gradual. The dominant tree species in and around the avalanche path is Douglas-fir *Pseudotsuga menziesii* ((Mirbel) Franco), with quaking aspen *Populus tremuloides* (Michx), lodgepole pine *Pinus contorta* (Dougl.) and western larch *Larix occidentalis* (Nutt) also present.

Above the railroad, the Shed 10.7 path lies within GNP (est. 1910). Park management policies limit human activities within the path and thus the potential for human-caused tree damage that could be mistakenly attributed to avalanches. Wildfires that could affect a tree-ring record from the path include a large, stand-replacing wildfire in 1910 and several smaller wildfires in the 1920s (Barrett, 1986). Scars and charcoal were evident on some dead trees found in the forest west of the avalanche path, and the oldest tree sampled for this study dated to 1910. A high-volume runoff event that could affect the tree-ring record occurred in 1964, when record floods heavily damaged the railroad and highway in Stevens Canyon.

Regular observations by the authors since 2001 confirm the results of a previous analysis of historic avalanche events (Reardon et al., 2004), which indicate that natural avalanches in Stevens Canyon result almost exclusively from a distinct synoptic weather pattern. In this pattern, outbreaks of Arctic air flow west over the Continental Divide into Stevens Canyon. Warm, moisture-laden Maritime air masses then ride over the denser, colder air. Initially, lifting of the Maritime air causes sustained snowfall. Eventually, as the Maritime air pushes the Arctic air back east of the Divide, rapid and dramatic warming occurs, often accompanied by rain at mountain-top elevations. The rapid warming and rain trigger widespread natural avalanches that deposit debris into the runout zones.

Secondary mechanisms for triggering natural avalanches in Stevens Canyon are rapid windloading and solar radiation (Reardon, unpublished data). Avalanches observed to result from windloading have run only to mid-track. Intense solar radiation triggers some wet snow avalanches, particularly in March and April. These occur mostly in the avalanche paths with lower elevation start zones. When wet snow avalanches occur in the upper elevation start zones like Shed 10.7, the debris stops well above the runout zone.

Methods

HISTORIC RECORD

Reardon et al. (2004) compiled a 94-year chronology of historic avalanches in Stevens Canyon that includes 13 avalanche events known to have occurred in the Shed 10.7 path (Table 1). Sources consisted of personal interviews and historic documents and photographs from GNP, the Great Northern Railway, Montana Department of Transportation, and local newspapers. The historic record also includes 15 other avalanche events that we classified as possibly occurring in the Shed 10.7 path. Possible avalanche events were those for which the record indicated an avalanche occurred in the immediate vicinity of Shed 10.7 but the evidence was insufficient to confirm Shed 10.7 as the precise location, or those for which the record listed multiple avalanches within the canyon on a given date but did not give locations.

SAMPLE COLLECTION

We sampled 109 trees located in the lower track and upper runout zone of the Shed 10.7 avalanche path between the railroad

TABLE 1

Avalanche years identified using the selection criteria that integrate information from the historic record and the tree-ring record. Number and percentage of sample event-responses from tree rings ranked as high- (1–3) or low-quality (4–5) using the Tree-Growth Response Rating System are listed along with the dated avalanche winters and sample depth (*n*) . A "possible" classification under the "In Historic Record" column indicates avalanche activity was recorded that winter within Stevens Canyon, but its location could not be confirmed as Shed 10.7.

Year	In Historic Record	# Ranked 1–3	# Ranked 4–5	% Ranked 1–3	% Ranked 1–5	Sample Depth (*n*)
1912	Yes	0	0	0	0	1
1914	Yes	0	0	0	0	1
1919	Yes	0	0	0	0	2
1921	Yes	0	0	0	0	2
1922	Yes	0	0	0	0	2
1923	Yes	0	0	0	0	2
1929	Yes	0	0	0	0	7
1933	Yes	2	2	22	44	9
1935	Yes	0	0	0	0	9
1947	Yes	3	0	14	14	22
1950	Possible	10	3	42	54	24
1957	Yes	3	0	10	10	31
1966	Possible	8	3	17	24	46
1970	No	8	9	14	30	57
1974	No	6	9	9	22	69
1976	No	3	8	4	14	77
1979	Possible	3	7	4	12	86
1982	Possible	18	9	18	27	101
1983	Possible	7	13	7	20	102
1985	Possible	9	14	9	22	103
1987	Possible	4	8	4	12	104
1989	No	4	12	4	15	104
1990	Possible	8	9	8	16	104
1993	No	30	24	29	52	104
1997	Yes	13	4	13	17	103
2002	Possible	34	13	48	66	71
2003	Yes	7	3	14	20	49

and the bottom of the S-curve (Fig. 2a). Three types of samples were collected: (1) cross sections from dead trees (Fig. 3), (2) cross sections from the dead leaders of avalanche-damaged but still living trees, and (3) cores from living trees. GPS coordinates with <1 m accuracy were recorded for each sampled tree using a Trimble GeoExplorer XT®. Notes described the amount of impact scarring, branch flagging, tilting, and other salient characteristics of each sampled tree.

Sample types (1) and (3) were collected as close to the root buttress as possible. This practice provides accurate estimates of establishment dates and captures reaction wood (i.e. colored wood tissues produced when a tree responds to impact or tilting with asymmetrical growth). For all three types, we sampled visible scars that appeared to result from the impacts of avalanche debris. These scars were on the upslope sides of tree stems in line with the likely flow of avalanche debris and within 2 m of the bole of the tree. Both practices reduced the possibility of including rockfall-induced growth responses in the chronology because rockfall-induced injuries tend to be scattered vertically and radially on tree stems (Stoffel, 2006). Samples were collected at random from the majority of available *in situ* trees of all species within and along the margins of the Shed 10.7 avalanche path. No samples were collected below the snowshed or railroad, where railroad and highway maintenance and other human activities have damaged trees, resulting in growth responses that could be mistakenly ascribed to avalanches.

FIGURE 3. *In situ* tree with cross-section sample and GPS unit for recording location.

Cross sections were collected from 67 dead, *in situ* trees and comprise the majority (62%) of our samples (Fig. 3). These samples came from trees with intact root wads and trunks that were oriented roughly parallel to the flow path of the slope, indicating they were likely killed in an avalanche. A smaller number of cross sections ($n = 24$; 22%) were collected from the dead leaders of avalanche-topped trees where cambial growth was still active. This technique maximized data collection from frequently impacted living trees in the lower track of the avalanche path while avoiding damage due to sampling. Lastly, 18 live trees (16%) showing obvious avalanche damage (e.g. tilting, impact scarring, and branch flagging) were sampled using an increment borer. Four cores were removed from each tree, two perpendicular and two parallel to the fall-line of the slope. This procedure helped in the detection of growth anomalies and reaction wood in core samples.

SAMPLE PROCESSING AND ANALYSIS

All samples were processed using standard dendrochronology procedures (Stokes and Smiley, 1968). Missing and/or false rings were accounted for, and accurate dating was statistically verified using the COFECHA program (Grissino-Mayer et al., 1997). Initial crossdating of samples using a local reference chronology (Park Creek) was performed on all but the most heavily impacted samples. The Park Creek chronology was constructed from increment cores collected from 20 Douglas-fir trees ($n = 34$ individual series) the year prior to this study (2003). The site was located 14 km north of the Shed 10.7 path on a slope of similar elevation and aspect (Pederson and Littell, unpublished data). For samples heavily impacted by multiple avalanches, avalanche "marker years" recorded in neighboring samples (e.g. 1993 and 2002 avalanche events) ensured accurate calendar dating.

We then rated each avalanche-induced growth response/injury from 1 to 5 based on the visual quality of scars or reaction wood within each sample. This tree-growth response rating system is similar in concept to systems utilized in recent dendrogeomorphological studies by Luckman and Frazer (2001) and Germain et al (2005). Such systems allow the data to be filtered by sample quality during analysis, and the analysis results to be verified. The system used in this study is outlined below:

(1) Clear impact scar associated with obvious reaction wood or growth suppression.

(2) Clear scar, but no reaction wood or suppression of growth, or, obvious reaction wood/suppression of growth that occurs abruptly after complacent or "normal" growth and that lasts for approximately 3 years.

(3) Well-defined reaction wood/suppression of growth, but only prevalent in 1 or 2 successive growth years.

(4) Reaction wood or growth suppression present but not well defined, or, reaction wood present but formed when tree was young and more susceptible to damage from various environmental and biological conditions.

(5) Same as (4) except reaction wood is very poorly defined, and slow onset may indicate other processes such as soil or snow creep may be primary causes.

Once the quality of recorded events was assessed, event-response histograms were produced following Shroder (1978) and Dube et al. (2004). Two histograms were calculated by using (1) the raw number and (2) the percentage of trees (calculated from total number of living trees in year t) recording an event through growth responses (Fig. 4). Thus, the index I is calculated for each year t as follows:

$$I_t = \left(\left(\sum_{i=1}^{n} Rt \right) \div \left(\sum_{i=t}^{n} At \right) \right) \times 100 \qquad (1)$$

where R represents a tree's response to an event in year t, and A is equivalent to the number of trees alive in that year t (equation reproduced from Shroder, 1978). Following Dube et al (2004), we required that 10 or more trees exhibit a response and that the index I be $\geq 10\%$ of the samples alive at year t in order to classify an event as an avalanche year based solely on growth responses. The first threshold reduced the potential for overestimation—noted by Dube et al. (2004)—that can occur with decreased sample size early in the record. The second minimized the chance that growth anomalies caused by environmental factors and other geomorphological processes such as rockfall would mistakenly be ascribed to avalanches. A year was automatically classified as an avalanche year if the historic record listed a known avalanche in Shed 10.7 that winter.

CALCULATIONS OF NATURAL AVALANCHE RETURN PERIODS AND EXTENT

Avalanche frequency is the average time interval within which debris reaches a given point in an avalanche path (McClung and Schaerer, 1993). Frequency is usually expressed in years as a "return period" (1/frequency). For this study, we calculated return periods for each tree within the path and then for the entire lower section of the path by combining the individual tree return period estimates with the spatial data in ArcMap 9.2 (ESRI, 2005). Individual tree return periods were calculated from the growth response frequency f for each tree T as follows:

$$f_T = \left(\sum_{i=T}^{n} Gr \right) \div \left(\sum_{i=T}^{n} A \right), \qquad (2)$$

where Gr represents the number of growth responses, and A the total number of years tree T was alive.

Return Periods were next mapped using a standard sequence of kriging methods to ensure robust spatial estimates. (For more examples and details on the use of this method see Fortin and Dale, 2005; and Marinoni, 2002; Rossi et al., 1992.) In general, all kriging methods use spatial data within a set neighborhood to estimate the value of a variable of interest in a location where it has not been measured (Fortin and Dale, 2005). First, exploratory visualizations of avalanche return periods were performed using an interpolation method known as inverse distance weighting. This step (not presented here) helped ensure interpolated avalanche frequency patterns produced using the kriging method did not result solely from parameterization of the model by allowing for visualization of spatial structure in the raw point data. Next, the distribution of the data, along with the spatial autocorrelation structure between trees across the landscape, was used to inform the final model, which resulted in spatially accurate estimates of avalanche return periods. Here, the best-fit model of avalanche return periods was produced using the ordinary kriging approach and a spherical semivariogram. Using the spatial autocorrelation between points and the distribution of data, the lag (or bin) size was set to 27.75 m with 12 lags to optimize the fitting of the semivariogram. Due to the strong directional influence (i.e. points are closely related to those upslope of their location), anisotropy was set using an angle direction of 0° (approximately due north), an angle tolerance of 45°, and a bandwidth of 6. For estimating the avalanche frequency of a point on the landscape, an ellipse-shaped search neighborhood used at least 5 and up to 25 weighted points within each of its eight sectors.

The validity of the spatial model of avalanche return periods was confirmed using several standard methods. First, exploration of the raw data indicated the assumptions required for statistically valid modeling (e.g. normal distribution) were met. Then, model skill was assessed by looking at the difference, or error, between predicted and observed values using a cross validation technique similar to the 'leave-one-out' method. In this process, the entire data set was used, but each individual point was sequentially omitted and its value predicted using the remaining data. The difference between the predicted and observed values at each point provided a realistic estimate of model error, and consequently information as to whether the model was suitable for mapping. The error statistics generated for the spatial map of avalanche return periods indicate a high level of model skill and acceptable levels of model error (Table 2)

The database of sample locations, and thus growth responses by year, was also used to investigate questionable avalanche years,

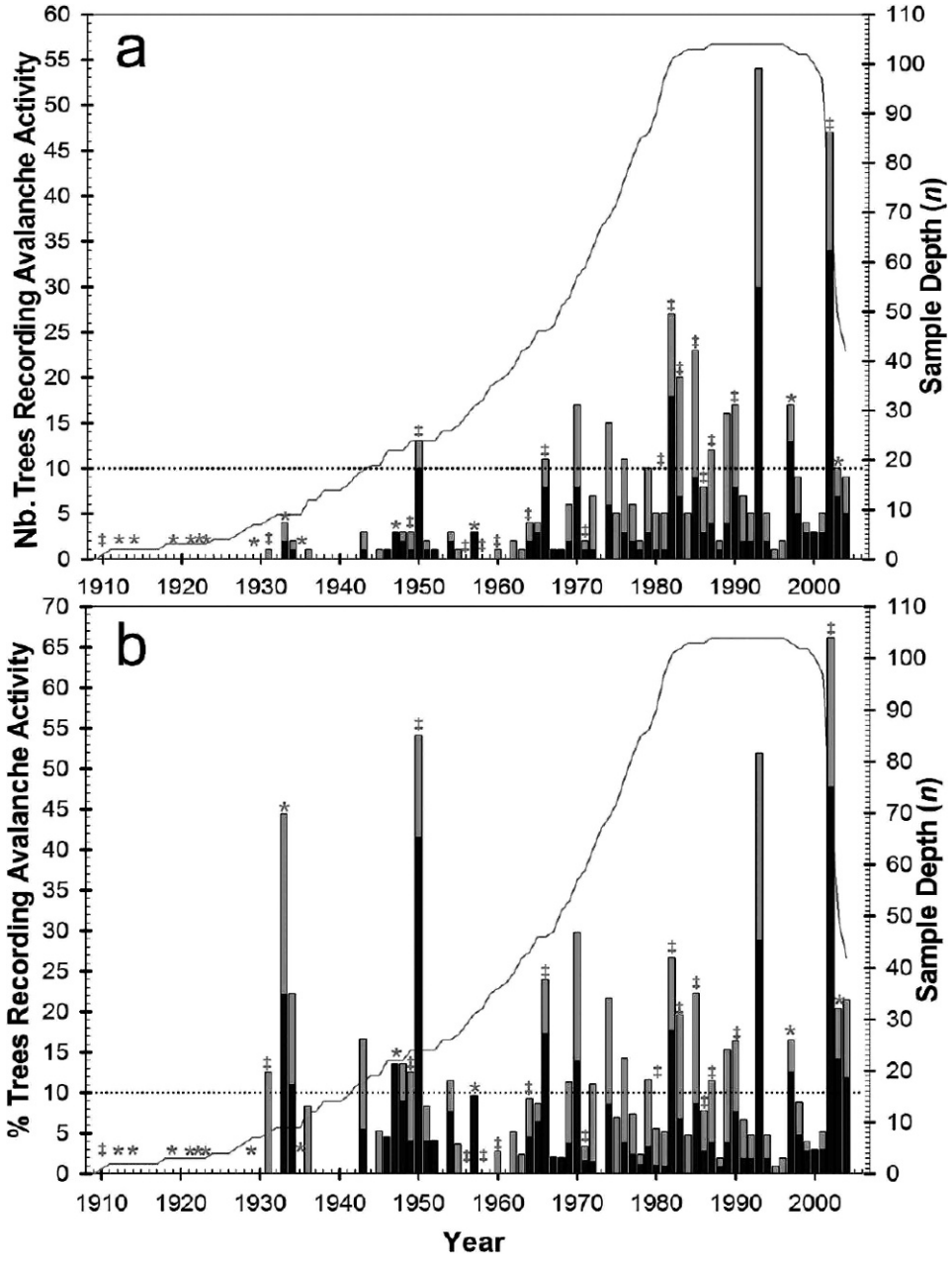

FIGURE 4. Event-response histograms showing the dated scars or reaction wood from sampled trees, and historic avalanche events. (a) Total number of trees, and (b) the percentage of trees responding to a damage event. Stacked bar graphs show the proportion of samples classified as high- (1–3, dark shading) and low-quality (4–5, light shading) using the tree-growth response rating system. Horizontal dotted line demarcates, in (a), the $n \geq 10$ tree threshold, and, in (b), the 10% of sample depth thresholds. The gray line shows the total number of trees (n) alive each year. Avalanche events known from the historic record are identified using a star and possible avalanche events with a ‡.

and to estimate minimum slide extent for each year classified as an avalanche event. Minimum slide extent estimates were developed by mapping all trees showing and not showing growth responses in the specific avalanche year. Maps of growth responses for years close to the 10% or 10 trees thresholds were examined to determine whether the growth responses showed a spatial pattern consistent with avalanche runout or more random events such as rockfall.

AVALANCHE AND CLIMATE RELATIONSHIPS

Lastly, we compared the avalanche chronology with snowfall data and synoptic climate indices to look for associations between climate and natural avalanche frequency and extent. The primary meteorological parameter was annual 1 March snow water equivalent (SWE; 1935–2003) for the Marias Pass snow course (USDA, 2006), located on the Continental Divide 16 km northeast of Shed 10.7. The Marias Pass record provides snowfall data representative of canyon-wide conditions over a period of record that best matches the Shed 10.7 avalanche history. Because the majority of avalanches in Stevens Canyon occur in January and February (Reardon et al., 2004), we used 1 March SWE anomalies as a measure of snowfall for each winter.

Previous studies (Selkowitz et al., 2002; McCabe and Dettinger, 2002; Pederson et al., 2004) have linked snowfall in the region to the Pacific Decadal Oscillation (PDO) and, to a lesser extent, the El Niño–Southern Oscillation (ENSO) 3.4 region. Another study (Dixon et al., 1999) found that the frequency of large magnitude avalanches in the GNP region was reduced during El Niño years. We therefore briefly investigated the degree to which indices for these synoptic climate patterns correlate with natural avalanches in Shed 10.7. We used the mean of the monthly January–February indices (University of Washington, 2006; NCAR, 2006) as a measure of the cumulative strength of each index for each winter (1910–2003); these means had the highest correlations with 1 March SWE at the Marias Pass snow course and overlapped the two months in which avalanche activity in the canyon peaks (Reardon et al., 2004). As a measure of the relative

TABLE 2

Cross validation statistics and model error coefficients for the kriged return period map (Fig. 5). Models providing accurate predictive capabilities should exhibit mean error values close to 0, root-mean-squared error and standard error should as small as possible, and the root-mean-square standardized error should be close to 1.

Error Metric	Value
Mean	–0.0002301
Root-Mean-Square	0.0739
Average Standard Error	0.06809
Mean Standardized	–0.001213
Root-Mean-Square Standardized	1.072

strength of the multi-year climate patterns for each year, we ranked the means of each index for each year of the period. To facilitate comparisons, we then divided the rankings into thirds; we classified the lowest third as negative phase winters, the middle as neutral phase winters and the upper third as positive phase winters. We then used a non-parametric, two-sample *T*-test to determine whether any apparent coincidences were statistically significant at the 95% confidence interval.

Results

RECONSTRUCTED TREE-RING AVALANCHE RECORD

The oldest of the 109 samples dated to 1910 (Figs. 4a, 4b). In 1936 the sample size surpassed the $n \geq 10$ trees threshold for growth responses to be classified as an avalanche event using the tree-ring record alone. The sample size increased markedly after 1965 and surpassed 50% ($n = 55$) in 1972. The earliest growth response occurred in 1931, and the earliest responses that received high-quality scores (1–3) occurred in 1933 and 1934 when sample size was below the threshold of 10 trees. Only 1933 was classified as an avalanche year because historic records indicate avalanche activity that winter (Table 1). Growth responses became more frequent after 1936, and after 1960, nearly every year exhibited some responses by a small number of trees. Most of these years were not classified as avalanche years because fewer than 10 trees and less than 10% of the samples alive that year showed responses. Snow creep may account for many of these responses. Growth responses did exceed our classification thresholds in 18 years after 1936, and all of these were classified as avalanche years. Evidence for avalanches was particularly robust in 1950, 1993, and 2002, when more than 50% of the trees alive those years showed growth responses. Growth responses did not exceed the classification thresholds in 1964, the year of record floods in the region, and 1964 was not classified as an avalanche year.

COMBINED TREE-RING AND HISTORIC AVALANCHE CHRONOLOGY

Combining the tree-ring and historic records yielded a total of 27 avalanche years in the 94-year chronology (1910–2003), more than doubling the number of confirmed avalanches in Shed 10.7 over the historic record alone (Table 1). From 1910 to 1936, the tree-ring record showed growth-responses in only three years, with one of those coinciding with a known historic avalanche event ($n = 9$) and none coinciding with possible but unconfirmed avalanche events ($n = 2$). After 1936, the tree-ring record included growth responses that are ≥10% of samples in all known historic avalanche years ($n = 4$) and many years that were either possible but unconfirmed ($n = 9$), or absent from the historic record ($n = 5$). In all but two of these cases—known avalanche years 1947 and 1957—10 or more trees recorded growth responses. We removed six possible avalanche years from the avalanche chronology when <10 trees and <10% of the total samples alive that year recorded responses. All of those years but one—1986—were well below the thresholds. In 1986, 8 of 109 samples showed growth responses, with 3 of those scoring from 1 to 3.

The scores from the tree-growth response rating system confirmed the classification of event-responses as avalanche years. All 18 years after 1936 classified as avalanche years showed at least 3 samples with high-quality scores (Table 1; Figs. 4a, 4b), with a mean of 9.89 and a maximum of 34. These numbers represent a minimum of 4% and a mean of 14.9% of the samples available for each avalanche year. High quality scores (1–3) for each avalanche year indicated that there were multiple samples with clear physical evidence of avalanche-induced damage or growth responses for that year.

AVALANCHE RETURN PERIOD ESTIMATES AND MAPPING

The average return period for the entire sampled area of the Shed 10.7 path (Table 3) was calculated for four intervals: (1) 1910–2003, (2) 1910–1935, (3) 1936–2003, and (4) 1969–2003. The intervals were selected to cover (1) the entire length of the chronology (historic and tree-ring records), (2) the period in which sample depth was less than 10 trees but historic records were relatively detailed, (3) the period after sample depth reached $n \geq 10$ trees and for which snowpack records are available, and (4) the period during which more than 50% of the sampled trees were alive. For these four intervals, calculated return periods range from 2.5 to 3.8 years with an overall average of 3.2 years.

Within the sampled area of the Shed 10.7 path, return periods increased rapidly with distance downslope, particularly at the bottom of the debris fan immediately above the snowshed (Fig. 5). The map of avalanche frequencies within the sampled area showed calculated return periods ($1/f$) ranging from 2.3 years in the lower track to 25 years for the unprotected section of the railroad in the runout zone. The horizontal distance between these points is less than 300 m, with an elevation change of only 125 m. In the upper 40 vertical meters of the runout zone, return periods increased by only a year, from 4.8 to 5.9 years, yet nearly doubled in the remaining 50 vertical meters above the snowshed, to 11.1 years.

COMPARISON OF AVALANCHE CHRONOLOGY WITH SNOWPACK AND CLIMATE ANOMALIES

A comparison of the avalanche chronology with snow course data shows avalanche years are clearly associated with positive snowpack anomalies (Fig. 6). During the period 1936–2003, when historic and tree-ring avalanche records overlap with snowpack records, we identified 18 avalanche years. The number of years with positive ($n = 34$) and negative ($n = 34$) 1 March snowpack anomalies was equal. Avalanche years coincided with positive snowpack anomalies in 11 years (32.4%) and with negative snowpack anomalies in seven years (20.6%) (Table 4). Snowfall and avalanche relationships were more sharply defined when a buffer was used to account for average snowpack conditions. The buffer classified as average any year that SWE values were ±10% (3.8 cm) of the mean for the 1935–2003 snowpack data. Avalanche years corresponded to 36% and 31.3% of the years of positive ($n = 25$) or average ($n = 16$) snowpack, respectively.

TABLE 3

Return periods for four intervals in the reconstructed Shed 10.7 avalanche path chronology. The four intervals cover the entire length of record (both historic and tree-ring based), the years early in the chronology when the historic record is detailed but tree-ring data is limited, the years for which sample depth is $n \geq 10$ trees and snow water equivalent data is available from Marias Pass, and the years when tree-ring data is abundant but historic data is scarce.

Interval	# Years	# Avalanches	Return Period (yr)
1910–2003	94	27	3.5
1910–1935	25	9	2.9
1936–2003	68	18	3.8
1969–2003	35	14	2.5
		Average:	3.2

However, avalanches were recorded in only 14.8% of years with negative snowpack ($n = 27$).

A comparison of 1 March SWE anomalies at Marias Pass showed a strong negative correlation (–0.62) with mean Jan.–Feb. PDO indices, and a weaker negative correlation (–0.37) with mean Jan.–Feb. indices for the Niño 3.4 region (Table 5). However, a similar comparison of the climate indices with the Shed 10.7 avalanche chronology showed weak associations with the neutral phases of the PDO and Niño 3.4 indices (Table 6). For the 1910–2003 period of the study, 11 of the 27 avalanche winters coincided with the middle third of the mean Jan.–Feb. PDO and Niño 3.4 scores. The remaining avalanche winters were closely divided amongst PDO and Niño 3.4 positive and negative phases. Avalanches were slightly more frequent during PDO negative and Niño 3.4 positive phases. Despite these coincidences, the results of the Mann-Whitney non-parametric two sample *T*-tests showed no significant difference between the 1 March SWE totals for avalanche years and non-avalanche years, and no significant differences in the PDO and ENSO 3.4 indices for avalanche years and non-avalanche years.

Mapping of minimum avalanche extent in avalanche years showed little relationship between spatial extent of avalanche debris and 1 March snowpack anomalies. Figure 7 shows reconstructed minimum avalanche extent for four years as examples. Year 1950 was identified from the historic record as a possible avalanche year and confirmed by the tree-ring record. Years 1970 and 1993 were identified solely from the tree-ring record, whereas 1997 was documented in the historic record. The avalanche events of 1950 and 1997 were associated with strongly positive 1 March snowpack anomalies at the Marias Pass snow course, where data showed +23.1 and +28.7 cm of SWE respectively (Fig. 6). In the 1950 event, sample size was low, but the event-response map clearly indicates an avalanche event that extended to the western edge of the debris fan and may have hit the railroad below. In contrast, the 1997 avalanche event stopped midway across the debris fan, well above the 1950 event. The 1970, 1993, and 2003 (not shown) avalanche years coincided with average to below average snowpack conditions, yet mapped avalanche extent was similar to or greater than 1997, ranging from the middle of the runout zone to just above the snowshed. Years

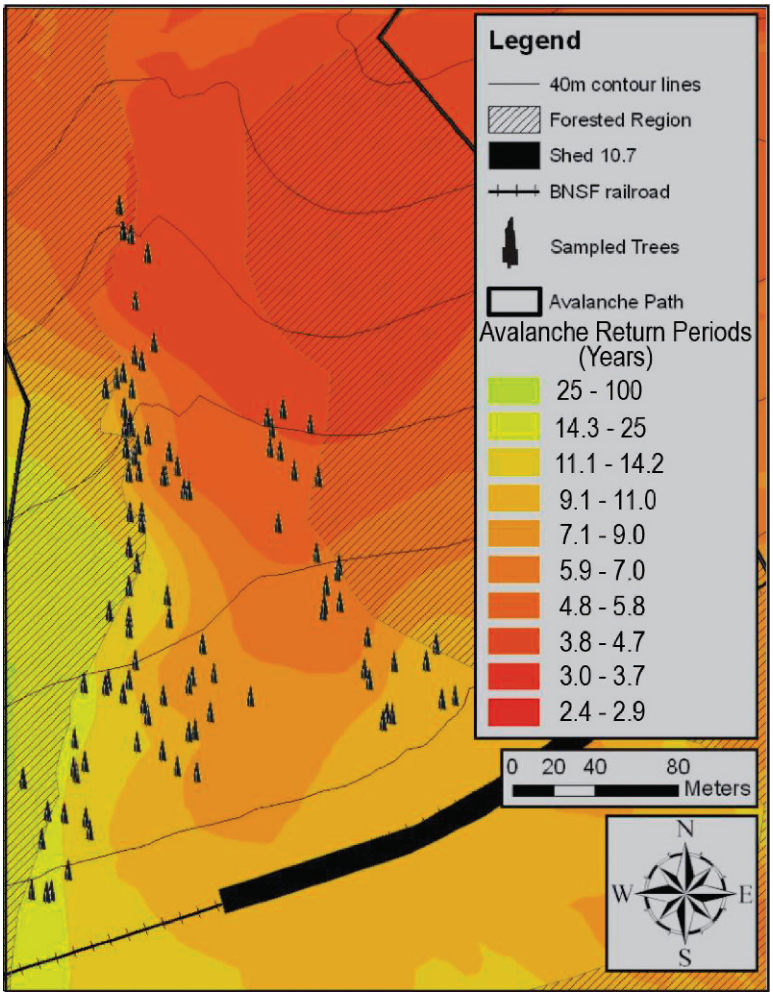

FIGURE 5. Interpolated return periods for the sampled area of the Shed 10.7 runout zone.

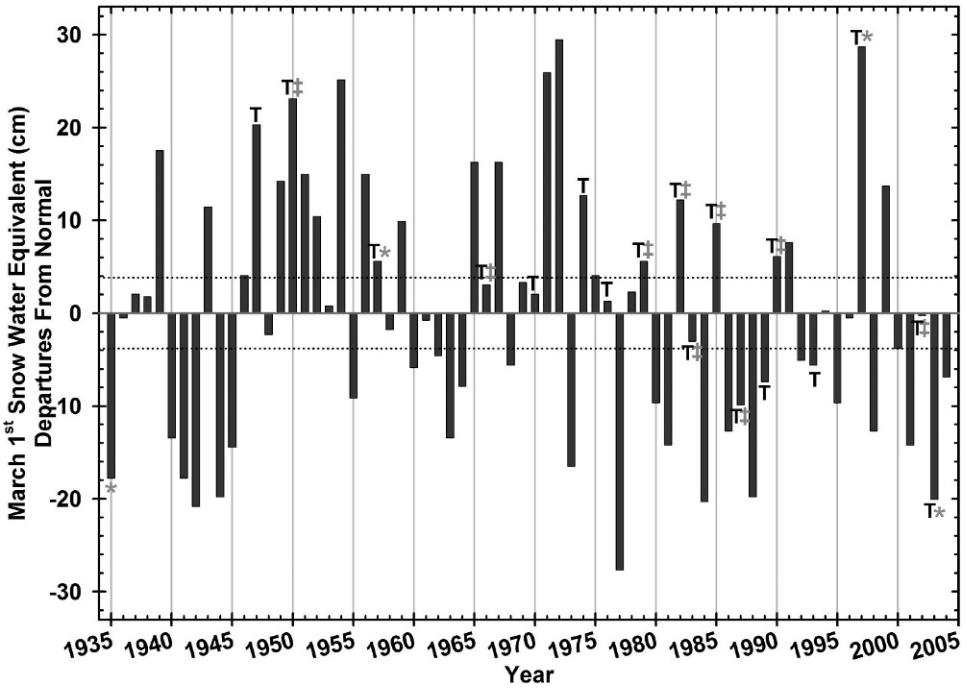

FIGURE 6. Marias Pass 1 March Snow Water Equivalent (SWE) departures from 1935 to 2004 mean and reconstructed/historic avalanche events for the Shed 10.7 avalanche path. All SWE values falling within ±3.81 cm (10% departure from normal) of the long-term mean are classified as neutral anomalies (dotted black line), and departures ≥ or ≤ this value are classified as positive or negative anomalies respectively. Avalanche events determined from tree-ring growth responses (see Table 1) are marked with a T, and an * or ‡ indicates a known or possible avalanche event in the historic record, respectively.

1970 and 1993 had average or mildly negative 1 March snowpack conditions (+2.0 and –4.6 cm SWE anomalies, respectively), while 2003 was strongly negative at –20.1 cm. Because the earliest samples from the eastern edge of the runout zone date from 1957, maps prior to this date show minimum avalanche extent only on the western side of the runout zone.

Discussion

ACCURACY OF THE SHED 10.7 AVALANCHE CHRONOLOGY

The tree-ring record expanded the avalanche chronology in the Shed 10.7 path from 13 to 27 known avalanche years. It confirmed 9 of the 15 possible avalanche years identified from the historic record, and added 5 previously unknown avalanche years to the chronology. Thus, combining tree-ring and historic records created a more complete and accurate chronology of natural avalanche activity than if either record were used alone.

The tree-ring and historic records each captured different periods at higher resolution (Figs. 4a, 4b; Table 1). From 1910 to 1935, railroad documents are particularly detailed and include nine avalanche years, while sample size for the tree-ring record in the same period was low ($n < 10$) and shows just one avalanche year. We suspect that few trees were growing in the runout zone during this period due to the 1910 wildfire, and those trees that were growing would likely have had small, flexible stems, which would minimize injury from avalanche debris. Many of the trees that reestablished after the 1910 wildfire may also have been destroyed by subsequent avalanches. In contrast, the latest part of the chronology (1969–2003) includes 14 avalanche years in the tree-ring record yet just two known avalanche years in the historic record. The discrepancy again appears to result from differences in the quality of the records. Sample size in the tree-ring record contained more than 50% ($n = 55$) of all trees sampled for most of this period, but historic documents were incomplete or vague. Both records showed the fewest avalanche years ($n = 4$) in the middle of the chronology (1936–1968). Sample size during this period was relatively low (10–43 trees) and fewer sources have been found from which to compile the historic record.

Several elements of the study methodology reduced the likelihood that growth responses due to non-avalanche events could be included in the chronology. These elements are consistent with recent findings that non-avalanche processes affect fewer trees or result in a spatial pattern of growth responses different than that caused by avalanche debris (Stoffel et al., 2006). Rockfall events, for example, have been distinguished from snow avalanches and debris flows by a more random distribution of growth responses amongst fewer trees (Stoffel and Perret, 2006). The possibility that anthropogenic tree damage would be mistaken for avalanche-induced injuries was minimized by only sampling trees above the railroad, where GNP management policies have severely restricted human activities since 1910. The two thresholds (≥10% of samples and ≥10 trees) helped screen out growth responses due to other environmental or geomorphic processes such as snow and soil creep, rockfall and high-volume runoff events that would affect only a limited number of trees on the site each year. Because growth responses in 1964, the year of record floods in the canyon, did not exceed the two thresholds, we infer that smaller volume, undocumented events would be unlikely to damage enough trees to exceed the thresholds. Many of these events could be expected to be concentrated in the shallow, tree-

TABLE 4

Number of winters and number of winters with avalanche events associated with positive, negative, or average snowpack anomalies. Calculations were performed with and without a buffer, which classifies snow conditions as average if SWE values fall within ±10% of the 1935–2004 mean.

Snowpack Anomaly	Winters, 1936–2003	Avalanche Winters, 1936–2003	Winters, 1936–2003 (w/buffer)	Avalanche Winters, 1936–2003 (w/buffer)
Positive	34	11 (32.4%)	25	9 (36%)
Average	—	—	16	5 (31.2%)
Negative	34	7 (20.6%)	27	4 (14.8%)

TABLE 5

Correlation between 1 March Marias Pass snowcourse measurements of SWE and snow depth, and the Pacific Decadal Oscillation (1910–2003) and Niño 3.4 (1910–2001) indices.

	Jan		Feb		Jan–Feb	
	PDO	Niño 3.4	PDO	Niño 3.4	PDO	Niño 3.4
SWE	–0.562	–0.378	–0.617	–0.355	–0.615	–0.368
p-value	*0.000*	*0.002*	*0.000*	*0.003*	*0.000*	*0.002*
Depth	–0.503	–0.411	–0.634	–0.381	–0.594	–0.398
p-value	*0.000*	*0.001*	*0.000*	*0.001*	*0.000*	*0.001*

less gully that bisects the runout zone and in which no samples were collected.

For years in which growth response exceeded these thresholds, two other analytical checks—the tree growth response rating system and spatial mapping of growth responses by year—allowed us to verify that those growth responses were avalanche-induced. The first ensured that there was clear physical evidence of injury and/or growth responses for each year identified as an avalanche year, and the second allowed us to check that growth responses were distributed in a pattern consistent with avalanches rather than randomly, as would be expected with rockfall (Stoffel and Perret, 2006). The mapping also allowed for a minimum threshold or Index Response identical to or higher than that used in other recent work (Dube et al., 2004; Germain et al., 2005), rather than the 40% suggested in older studies (Butler et al., 1987; Bryant et al., 1989). While the methodology minimizes the chances of including non-avalanche events in the chronology, it likely creates a bias towards larger avalanches; smaller avalanches that were confined to the shallow, tree-less gully in the runout zone would leave insufficient evidence to be captured by our sampling and analyses procedures. We thus conclude that our results constitute an accurate minimum chronology of natural avalanches of sufficient magnitude to have ecological impacts, those of approximately Destructive Class 2.5 or larger (McClung and Schaerer, 1993).

The results also underscore the inadequacy of relying on one type of record alone, as well as the value of long-term records of avalanche activity. A comparison between historic and tree-ring records in Shed 10.7 suggests that the historic record underestimates years with natural avalanches by roughly half. Yet while the tree-ring record may be a higher resolution record, it is also shorter term, covering roughly 30–50% of the historic record in detail because wildfires and larger avalanches periodically destroy trees in the runout zone, and thus much of the evidence of previous avalanche activity.

TABLE 6

Number of winters with avalanche events associated with positive, negative, or neutral Pacific Decadal Oscillation (PDO) and El Niño–Southern Oscillation (ENSO) conditions. The total number of winters associated with classified PDO or ENSO anomalies are also provided.

Dec.–Feb. Mean Index	PDO Winters, 1910–2003	PDO Avalanche Winters, 1910–2003	Niño 3.4 Winters, 1910–2001	Niño 3.4 Avalanche Winters, 1910–2001
Positive	31	7 (22.6%)	31	8 (25.8%)
Neutral	32	11 (34.4%)	30	11 (36.7%)
Negative	31	9 (29%)	31	6 (19.4%)

CALCULATED AVALANCHE FREQUENCIES AND MINIMUM AVALANCHE EXTENTS

The chronology and return periods resulting from this study can serve as a benchmark for evaluating return periods developed in other studies of the Shed 10.7 path and other avalanche paths in Stevens Canyon. At the elevation of the railroad and snowshed in the Shed 10.7 path, the return periods calculated through the kriged model (11.1 to 25 years) are longer than the return period of 10 years estimated by Hamre and Overcast (2004) for the same location from combined historic and tree-ring data. Methodological differences likely account for much of the differences in return periods, as Hamre and Overcast did not sample very far above the snowshed and collected only increment cores. This study's average return period for the sampled area in the Shed 10.7 path (3.2 years) is similar to return periods (3.4 and 6.1 years) derived from tree-ring based studies by Butler and Malanson (1985a, 1985b) of two other paths in Stevens Canyon. The similarities in return intervals suggest that avalanche activity in Shed 10.7 is typical of that throughout Stevens Canyon. However, the mapping element included in this study's methodology allowed for spatially precise estimations of return periods throughout the runout zone, rather than one average for multiple points in the path.

The maps of minimum avalanche extent for each avalanche year (Fig. 7) show that most avalanches in the path stop at similar elevations, but within that narrow elevation band the lateral extent of avalanches varies dramatically. The lateral variability of avalanche runout could result from meteorological factors, such as snowfall or windloading, that determine the amount of snow involved in natural avalanches, or from deflection that occurs when multiple avalanches run in a single winter and existing debris influences the direction of subsequent avalanche flow. Ecologically, the lateral variability in avalanche runout means disturbance varies spatially and temporally within short distances. This variability creates complex patterns of vegetation succession and structure in and around the Shed 10.7 avalanche path, increasing habitat diversity and other ecological benefits. If the Shed 10.7 path is representative of other paths in Stevens Canyon and the region, and natural avalanches are both frequent and spatially variable, then natural avalanches are, as disturbance agents, regular and significant contributors to the complexity and functioning of montane forests.

CLIMATE INFLUENCES ON NATURAL AVALANCHE FREQUENCY AND EXTENT

Our findings demonstrate a clear association between positive snowpack anomalies and natural avalanche frequency in the Shed 10.7 path. These snowpack anomalies are negatively correlated with PDO and ENSO, as shown in previous studies (Selkowitz et al., 2002; McCabe and Dettinger, 2002). From our findings,

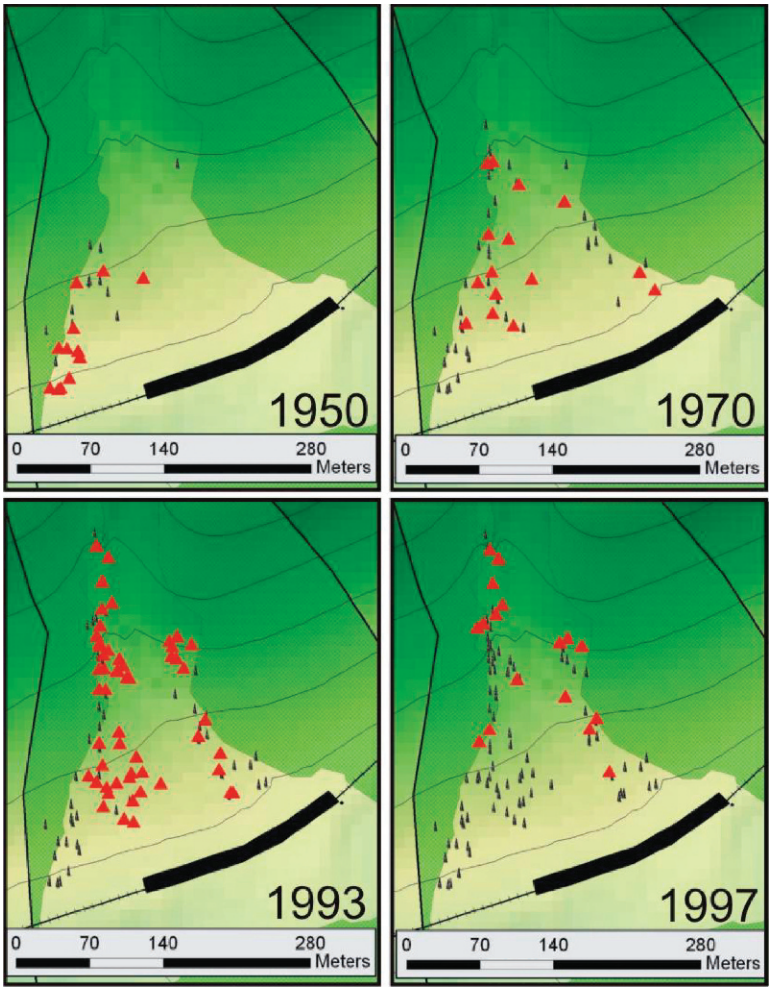

FIGURE 7. Reconstructed minimum slide extents for 1950, 1970, 1993, and 1997. Maps show total sample depth (conifer symbols) and all trees showing an event-response (red triangle) for the year of the avalanche.

however, it appears that there is little discernable relationship between multi-year climate anomalies and natural avalanche activity in the Shed 10.7 avalanche path. It may be that neither PDO nor ENSO influence the incursions of arctic air that are a key component of natural avalanche cycles in Stevens Canyon (Reardon et al., 2004) or that neither pattern promotes the distinct zonal or meridional flow identified as contributing to major avalanche winters in the region (Fitzharris and Schaerer, 1980; Butler and Malanson, 1986). Another explanation may be that for this particular avalanche path—or at the scale of any single avalanche path—natural avalanche activity is determined less by synoptic scale, multi-year climate patterns than by local topographic effects, the development of the snowpack over a winter, and short-term changes in meteorological factors such as precipitation intensity and temperature.

We suspect that at a larger spatial scale the association between multi-year climate patterns and anomalous snowfall does influence natural avalanche activity. Evidence for this suspicion includes the fact that 10 of the avalanche years established in this study correspond with avalanche years identified by Butler and Malanson (1985a) in two other paths in Stevens Canyon. The chronologies for all three paths overlap for the period 1922–1985, and four avalanche years are common to all three paths (1935, 1950, 1957, and 1979), with six more common to two of the three paths. Snowpack anomalies on 1 March at Marias Pass are positive for 6 of the 10 common winters, neutral for 2, and negative for 2. Likewise, mean Jan.–Feb. PDO scores are negative for 7 of the common avalanche winters, neutral for 1, and positive for 2. The common avalanche years are similarly biased towards winters with negative mean Jan.–Feb. Niño 3.4 scores, with 5 negative years, 4 neutral years, and only 1 positive year, supporting the tendency for fewer avalanches in the GNP region during El Niño winters reported previously (Dixon et al., 1999). The coincidence of positive SWE anomalies, negative PDO and Niño 3.4 indices, and winters with avalanche years common to two to three avalanche paths suggests that above-average snowfall driven by climate oscillations may result in more widespread avalanche activity throughout a winter, with correspondingly greater economic and ecological effects. If further study confirmed those associations, then natural avalanches are yet another mechanism through which climate has large scale and long-term ecological effects on montane forests.

Conclusion

This study presents results from a fairly unique avalanche research opportunity: a mountain area where avalanches are not controlled, in a national park where natural landscape responses can be studied, and within a key transportation corridor that provides easy access and whose existence has led to nearly a century of observations. The tree-ring analyses of the Shed 10.7 path added substantially to the historic record for this area, demonstrating the value of the approach. The findings indicated that ecologically significant avalanches occur at a higher frequency than is apparent solely from historic records, and that avalanches are associated with positive snowpack anomalies that may in turn

be correlated with multi-decadal climate patterns. Though additional analyses are needed to confirm the applicability of the findings to other avalanche paths in Stevens Canyon and GNP, this study points to the complex influence of climate on ecological patterns and processes in mountain environments. Changes in climate that alter snowfall totals would alter the frequency and/or minimum extent of natural avalanches and would thus have transformative effects on the montane forests and high-elevation landscapes of GNP. Such an outcome is of interest not only to ecologists, but also to park managers, railroad executives, highway planners, and avalanche workers, all of whom must anticipate avalanche potential on multi-year and multi-decadal scales.

Acknowledgments

We gratefully acknowledge support from the staff at Glacier National Park and the Big Sky Institute, Montana State University. We also thank two anonymous reviewers for comments and suggestions that helped improve the readability and presentation of the work. This work is a contribution of the US. Geological Survey Global Change Research Program's Western Mountain Initiative.

References Cited

Barrett, S. W., 1986: *Fire history of Glacier National Park: Middle Fork Flathead River drainage: final report*. West Glacier, Montana: National Park Service, Glacier National Park, 32 pp.

Baumann, F., and Kaiser, K. F., 1999: The Multetta debris fan, eastern Swiss Alps: a 500-year debris flow chronology. *Arctic, Antarctic, and Alpine Research*, 31(2): 128–134.

Braam, R. R., Weiss, E. E. J., and Burrough, P. A., 1987: Spatial and temporal analysis of mass movement using dendrochronology. *Catena*, 14: 573–594.

Bryant, C. L., Butler, D. R., and Vitek, J. D., 1989: A statistical analysis of tree-ring dating in conjunction with snow avalanches: comparison of on-path versus off-path responses. *Environmental Geological Water Science*, 14(1): 53–59.

Burrows, C. J., and Burrows, V. L., 1976: Procedures for the study of snow avalanche chronology using the growth layers of woody plants. Boulder: University of Colorado, Institute of Arctic and Alpine Research, *Occasional Paper*, 23: 54 pp.

Butler, D. R., 1986: Spatial and temporal aspects of the snow avalanche hazard, Glacier National Park, Montana, U.S.A. *In Proceedings of the International Snow Science Workshop, Lake Tahoe, California*, 223–230.

Butler, D. R., 1989: Snow avalanche dams and resultant hazards in Glacier National Park, Montana. *Northwest Science*, 63: 109–115.

Butler, D. R., and Malanson, G. P., 1985a: A history of high-magnitude snow avalanches, southern Glacier National Park, Montana, U.S.A. *Mountain Research and Development*, 5: 175–182.

Butler, D. R., and Malanson, G. P., 1985b: A reconstruction of snow avalanche characteristics in Montana, U.S.A, using vegetative indicators. *Journal of Glaciology*, 31: 185–187.

Butler, D. R., and Malanson, G. P., 1986: Snow-avalanche hazards in Glacier National Park, Montana: meteorologic and climatologic effects. *Physical Geography*, 7: 72–87.

Butler, D. R., Malanson, G. P., and Oelfke, J. G., 1987: Tree-ring analysis and natural hazard chronologies: minimum sample sizes and index values. *Professional Geographer*, 39(1): 41–47.

Butler, D. R., Malanson, G. P., and Walsh, S. J., 1992: Snow-avalanche paths: conduits from the periglacial-alpine to the subalpine depositional zone. *In* Dixon, J. C., and Abrahams, A. D. (eds.), *Periglacial Geomorphology*. London: John Wiley and Sons, 185–202.

Carrara, P. E., 1979: The determination of snow avalanche frequency through tree-ring analysis and historical records at Ophir, Colorado. *Geological Society of America Bulletin, Part I*, 90: 773–780.

Dixon, R. W., Butler, D. R., DeChano, L. M., and Henry, J. A., 1999: Avalanche hazard in Glacier National Park: an El Niño connection? *Physical Geography*, 20(6): 461–467.

Dube, S., Filion, L., and Hetu, B., 2004: Tree-ring reconstruction of high-magnitude snow avalanches in the northern Gaspé Peninsula, Quebec, Canada. *Arctic, Antarctic, and Alpine Research*, 36: 555–564.

ESRI (Environmental Systems Research Institute), 2005: ArcGIS 9.2, Redlands, California (1992–2006).

Fantucci, R., and Sorriso-Valvo, M., 1999: Dendrogeomorphological analysis of a slope near Lago, Calabria (Italy). *Geomorphology*, 30: 165–174.

Fitzharris, B. B., and Schaerer, P. A., 1980: Frequency of major avalanche winters. *Journal of Glaciology*, 26: 43–52.

Fortin, M., and Dale, M., 2005: *Spatial Analysis: a Guide for Ecologists*. Cambridge: Cambridge University Press, 365 pp.

Germain, D., Filion, L., and Hetu, B., 2005: Snow avalanche activity after fire and logging disturbances, northern Gaspé Peninsula, Quebec, Canada. *Canadian Journal of Earth Sciences*, 42: 2103–2116.

Grissino-Mayer, H. D., Holmes, R. L., and Fritts, H. C., 1997: The International Tree-Ring Data Bank Program Library. Version 2.1, users' manual, Tucson, Arizona, 106 pp.

Hamre, D., and Overcast, M., 2004: *Avalanche Risk Analysis, John Stevens Canyon, Essex, Montana*. Girdwood: Chugach Adventure Guides, 74 pp.

Hebertson, E. G., and Jenkins, M. J., 2003: Historical climate factors associated with major avalanche years on the Wasatch Plateau, Utah. *Cold Regions Science and Technology*, 37: 315–332.

Jenkins, M. J., and Hebertson, E. G., 1994: Using vegetative analysis to determine the extent and frequency of avalanches in Little Cottonwood Canyon, Utah. *In Proceedings of the International Snow Science Workshop, Snowbird, Utah*, 91–103.

Jenkins, M. J., and Hebertson, E. G., 2004: A practitioner's guide for using dendroecological techniques to determine the extent and frequency of avalanches. *In Proceedings of the International Snow Science Workshop, Jackson, Wyoming*, 423–431.

Luckman, B. H., and Frazer, G. W., 2001: Dendrogeomorphic investigations of snow avalanche tracks in the Canadian Rockies. Unpublished paper presented at the International Conference on the Future of Dendrochronology, Davos, Switzerland, 22–26 September.

Mace, R. D., and Waller, J. S., 1997: Grizzly bear habitat selection in the Swan Mountains, Montana. *Journal of Wildlife Management*, 61(4): 1032–1039.

Malanson, G. P., and Butler, D. R., 1984: Avalanche paths as fuel breaks: implications for fire management. *Journal of Environmental Management*, 19(3): 229–238.

Marinoni, O., 2002: Improving geological models using a combined ordinary-indicator kriging approach. *Engineering Geology*, 69: 37–45.

Martinelli, M., 1974: *Snow Avalanche Sites: Their Identification and Evaluation*. U.S. Department of Agriculture, *Information Bulletin*, 360: 27 pp.

Martinelli, M., 1984: The Goat Lick Bridge avalanches of 1979 and 1982. *In Proceedings of the International Snow Science Workshop, Aspen, Colorado*, 198–207.

McCabe, G. J., and Dettinger, M. D., 2002: Primary modes and predictability of year-to-year snowpack variations in the western United States from teleconnections with Pacific Ocean climate. *Journal of Hydrometeorology*, 3: 13–25.

McClung, D. M., and Schaerer, P. A., 1993: *The Avalanche Handbook*. Seattle: Mountaineers, 271 pp.

Mears, A. I., 1992: Snow avalanche hazard analysis for land-use planning and engineering. Colorado Geological Survey, *Bulletin*, 40: 54 pp.

NCAR (National Center for Atmospheric Research, Climate and Global Dynamics Division), 2006: El Niño Southern Oscillation 3.4 index data (http://www.cgd.ucar.edu/). Data: (ftp://ftp.cgd.ucar.edu/pub/CAS/TNI_N34/). Last accessed 19 January 2007.

Patten, R. S., and Knight, D. H., 1994: Snow avalanches and vegetation pattern in Cascade Canyon, Grand Teton National Park, Wyoming, U.S.A. *Arctic and Alpine Research*, 26: 35–51.

Pederson, G. T., Fagre, D. B., Gray, S. T., and Graumlich, L. J., 2004: Decadal-scale climate drivers for glacial mass balance in Glacier National Park, Montana, USA. *Geophysical Research Letters*, 31: article L12203, doi: 10.1029/2004GL019770..

Rayback, S. A., 1998: A dendrogeomorphological analysis of snow avalanches in the Colorado Front Range, U.S.A. *Physical Geography*, 19(6): 502–515.

Reardon, B. A., Fagre, D. B., and Steiner, R. W., 2004: Natural avalanches and transportation: a case study from Glacier National Park, Montana, U.S.A. *In Proceedings of the International Snow Science Workshop, Jackson, Wyoming*, 582–597.

Rossi, R. E., Mulla, D. J., Journel, A. G., and Franz, E. H., 1992: Geostatistical tools for modeling and interpreting ecological spatial dependence. *Ecological Monographs*, 62(2): 277–314.

Schaerer, P. A., 1989: The avalanche hazard index. *Annals of Glaciology*, 13: 241–247.

Selkowitz, D. J., Fagre, D. B., and Reardon, B. A., 2002: Interannual variations in snowpack in the Crown of the Continent Ecosystem. *Hydrologic Processes*, 16: 3651–3665.

Shroder, J. F. Jr, 1978: Dendrogeomorphological analysis of mass movement on Table Cliffs Plateau, Utah. *Quaternary Research*, 9(2): 168–185.

Stefannini, M. C., 2004: Spatio-temporal analysis of a complex landslide in the Northern Apennines (Italy) by means of dendrochronology. *Geomorphology*, 63: 191–202.

Stoffel, M., 2006: A review of studies dealing with tree rings and rockfall activity: the role of dendrogeomorphology in natural hazard research. *Natural Hazards*, 39(1): 51–70.

Stoffel, M., and Beniston, M., 2006: On the incidence of debris flows from the early Little Ice Age to a future greenhouse climate: a case study from the Swiss Alps. *Geophysical Research Letters*, 33: article L16404.

Stoffel, M., and Perret, S., 2006: Reconstructing past rockfall activity with tree rings: some methodological considerations. *Dendrochronologia*, 24(1): 1–15.

Stoffel, M., Bollschweiler, M., and Hassler, G. R., 2006: Differentiating past events on a cone influenced by debris-flow and snow avalanche activity—A dendrogeomorphological approach. *Earth Surface Processes and Landforms*, 31(11): 1424–1437.

Stokes, M. A., and Smiley, T. L., 1968: *An Introduction to Tree-Ring Dating*. Chicago: University of Chicago, 73 pp.

USDA, 2006: Marias Pass snow course data (http://www.wcc.nrcs.usda.gov/). Last accessed 19 January 2007.

University of Washington (Joint Institute for the Study of the Atmosphere and Ocean), 2006: Pacific Decadal Oscillation data (http://jisao.washington.edu/pdo/PDO.latest). Last accessed 19 January 2007.

Walsh, S. J., Weiss, D. J., Butler, D. R., and Malanson, G. P., 2004: An assessment of snow avalanche paths and forest dynamics using Ikonos satellite data. *Geocarto International*, 19(4): 1–9.

Ms accepted February 2007